ADVANCED FUNCTIONAL MATERIALS
www.afm-journal.de

Thin Film Silicon Photovoltaic Cells on Paper for Flexible Indoor Applications

Hugo Águas, Tiago Mateus, António Vicente, Diana Gaspar, Manuel J. Mendes, Wolfgang A. Schmidt, Luís Pereira, Elvira Fortunato, and Rodrigo Martins**

The present development of non-wafer-based photovoltaics (PV) allows supporting thin film solar cells on a wide variety of low-cost recyclable and flexible substrates such as paper, thereby extending PV to a broad range of consumer-oriented disposable applications where autonomous energy harvesting is a bottleneck issue. However, their fibrous structure makes it challenging to fabricate good-performing inorganic PV devices on such substrates. The advances presented here demonstrate the viability of fabricating thin film silicon PV cells on paper coated with a hydrophilic mesoporous layer. Such layer can not only withstand the cells production temperature (150 °C), but also provide adequate paper sealing and surface finishing for the cell's layers deposition. The substances released from the paper substrate are continuously monitored during the cell deposition by mass spectrometry, which allows adapting the procedures to mitigate any contamination from the substrate. In this way, a proof-of-concept solar cell with 3.4% cell efficiency (41% fill factor, 0.82 V open-circuit voltage and 10.2 mA cm^{-2} short-circuit current density) is attained, opening the door to the use of paper as a reliable substrate to fabricate inorganic PV cells for a plethora of indoor applications with tremendous impact in multi-sectorial fields such as food, pharmacy and security.

1. Introduction

The next-generation of low-cost flexible, disposable, portable, and potentially wearable electronic systems will require the integration of energy power sources to turn them fully autonomous. These electronic systems are expected to attain a major influence in our future lifestyles at the levels of communications, logistics, and medicine. For this reason, it is highly demanding to develop thin, lightweight, and flexible energy sources with various sizes and shapes and capable of being integrated with such low-cost consumer-oriented systems.[1–3] Such sources can be constituted by a solid-state paper battery,[4,5] charged by a photovoltaics (PV) cell.

The technology and fabrication process of these energy sources must be compatible with large-scale and roll-to-roll manufacturing,[6–8] which yield the amenability to low-cost production, a requirement particularly important for disposable devices. This means that the substrate where they are fabricated will play a major role, as it should be compatible with such production processes. The properties of the substrate will ultimately determine if the device will be flexible or rigid, heavy or light, transparent or opaque and if it can be applied to roll-to-roll processing, today's most preferred industry manufacturing process.[9] So far, plastic substrates have dominated this technology mostly due to their flexibility, lightweight, durability, and widespread usage. Various types of electronics systems supported on plastic substrates have been reported,[10,11] particularly in the field of flexible displays. For power generation, the majority of flexible PV cells produced so far have also employed smooth plastic substrates, such as polyethylene terephthalate (PET).[12,13]

However, a major concern with plastics is that they have low thermal durability and a high coefficient of thermal expansion, which frequently becomes an obstacle for the manufacturing processes. High-quality plastics can alleviate these problems, but are expensive, and since the substrate occupies a large portion of the devices, cost-effective and environmentally friendly materials are strongly required.

1.1. Why Cellulose Paper as Substrate?

Cellulose paper has excellent mechanical properties, such as flexibility and foldability, and it is a low-cost, recyclable, and environmental friendly material.[14–16] It is chemically and mechanically stable under atmospheric conditions and its surface wetting properties can be easily modified.[17] Moreover,

Prof. H. Águas, T. Mateus, A. Vicente, D. Gaspar, Dr. M. J. Mendes, Prof. L. Pereira, Prof. E. Fortunato, Prof. R. Martins
CENIMAT/I3N, Departamento de Ciência dos Materiais
Faculdade de Ciências e Tecnologia
FCT, Universidade Nova de Lisboa
and CEMOP/UNINOVA
2829-516, Caparica, Portugal
E-mail: hma@fct.unl.pt; rm@uninova.pt
Dr. W. A. Schmidt
Schoeller Technocell GmbH & Co.KG
49086 Osnabrück, Germany

DOI: 10.1002/adfm.201500636

paper is quite stable at elevated temperature. The degradation of cellulose, the major constituent of paper, begins at a temperature above 250 °C, while its extensive degradation occurs when the temperature is over 300 °C.[18] Furthermore, cellulose can be obtained from various plants and represents one of the most abundant organic materials on earth.[14] As a consequence, there has been a recent increased interest in integrating low-cost and disposable electronics into paper substrates, including transistors, storage devices, displays, and circuitry.[14–16,19] Therefore, paper electronics is now considered to be the most likely technology to replace the currently used plastic-based electronics.

There are already a wide range of applications,[18,20] such as field effect transistors, [21] active matrix displays,[22] memory devices,[21] printed circuits,[23] self-rechargeable batteries,[4] CMOS[24] devices, biosensors,[25,26] organic photovoltaic devices,[27,28] touch sensors,[29] chemical and biological sensors,[3,18] to name a few examples, which have already been demonstrated on substrates made of paper or using even paper as an active component.

Paper-based photovoltaic (PV) devices are the ideal power source for most of the low-cost disposable electronic commodities based on the above-mentioned devices. In addition, they can contribute to the creation of new paradigms concerning light harvesting, including its seamless integration into ubiquitous formats such as window shades, wallpaper, wear, and magazines. Its installation may be as simple as cutting the paper PV to the desired size and then gluing it onto the required surfaces. From the cost point of view, paper substrates for PV applications are also remarkably attractive, as they are about 100 times less expensive than common plastic substrates (0.2–3 $ m^{-2}),[14,27] which is an important factor considering that the substrate represents 25%–60% of total material costs in current thin film PV modules.[27,30] Additional cost savings are anticipated to come from the combination of the paper low weight and its ability to achieve a compact form by rolling it. The application of paper substrates to inorganic PV devices is not straightforward, due to its characteristic surface roughness and porosity. That is why most paper PV applications have been so far related with the demonstration of organic PV cells with a relatively low efficiency.[31,32]

To the authors' knowledge, it has not yet been demonstrated the use of silicon thin film materials [33] or other inorganic materials on paper substrates for fabricating PV devices. Silicon thin film technology requires substrate surfaces free from microporosity that it is not fulfilled by standard papers, which have a relatively rough and porous surface due to their cellulose fiber structure. However, there are ways to overcome these drawbacks, such as smoothing the paper surface by coating followed by supercalendaring or even more effective cast-coating a layer,[34] which gives it a smooth finishing.[18,35,36] Smoothing the paper surface can decrease its wettability, which may be problematic for some printing applications, but can make it suitable to coating by PVD and CVD technologies. Silicon thin films, in particular hydrogenated amorphous silicon (a-Si:H), have the advantage of a high absorption coefficient (10^4–10^5 cm^{-1}) in the visible range[37] and a good capability to absorb diffused light, making it a preferential material for PV indoor applications, as the cells are capable of generating voltages close to their characteristic V_{OC} under indoor ambient light conditions. This characteristic is particularly useful for electronic applications that would require essentially voltage rather than current. Moreover, thin film silicon PV is a mature technology fully compatible with the roll-to-roll process,[8,38] and can be used to produce flexible PV cells that are bendable up to 10 mm curvature radius without loss of performance.[39] Current industrial roll-to-roll web speeds for amorphous silicon deposition by plasma-enhanced chemical vapor deposition (PECVD) are in the range of 72 m h^{-1}, for a deposition rate of 4–5 Å s^{-1}, as used in Xunlight Corporation module production.[40]

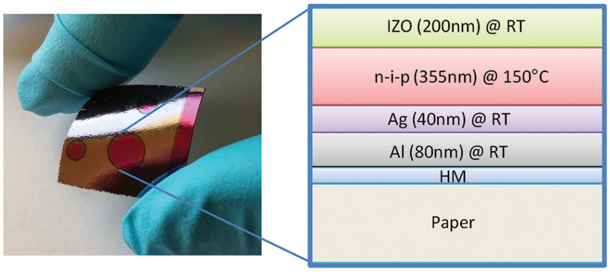

Figure 1. Photo of the a-Si:H PV cells on the FS-2 paper and schema of the layers that constitute the PV device.

This article presents a method that enables the production of thin film silicon PV devices on paper substrates, as a proof of concept. **Figure 1** shows a picture of the actual devices obtained on paper and a schema of its layers' structure.

For this purpose, we investigated the use of a printing paper ("p_e:smart Type 2," called FS-2 hereafter), developed by the German company "Felix Schoeller Group" that contains a cast-coated layer of a hydrophilic mesoporous (HM) material as a substrate[34] for a-Si:H cells deposition.

2. Paper Characterization

2.1. Morphological Analysis

The scanning electron microscopy (SEM) images depicted in **Figure 2** illustrate the difference between the surface morphology of the raw paper and the FS-2 paper after the cast coating process that forms the hydrophilic mesoporous (HM) surface. The raw paper (Figure 2a,b) consists of pressed cellulose fibers with several micrometers of diameter forming a network with the characteristic high porosity of paper. As mentioned above, this type of surface morphology forbids its use as a substrate for silicon thin film PV devices, since its high porosity would be a major cause of inhomogeneity and pinholes in the films having hundreds of nanometers, and consequently leading to poor device performance and low process yield.

The cast-coating of the HM layer modifies completely the paper surface morphology. Instead of cellulose fibers, a smooth surface with mesoporous of dimensions < 50 nm and with an average (RMS) roughness of 9.42 nm, determined by atomic force microscopy (AFM) analysis, is seen in Figure 2d. These mesopores are responsible for the good wetting properties (contact angle < 60°, see the Supporting Information) of the

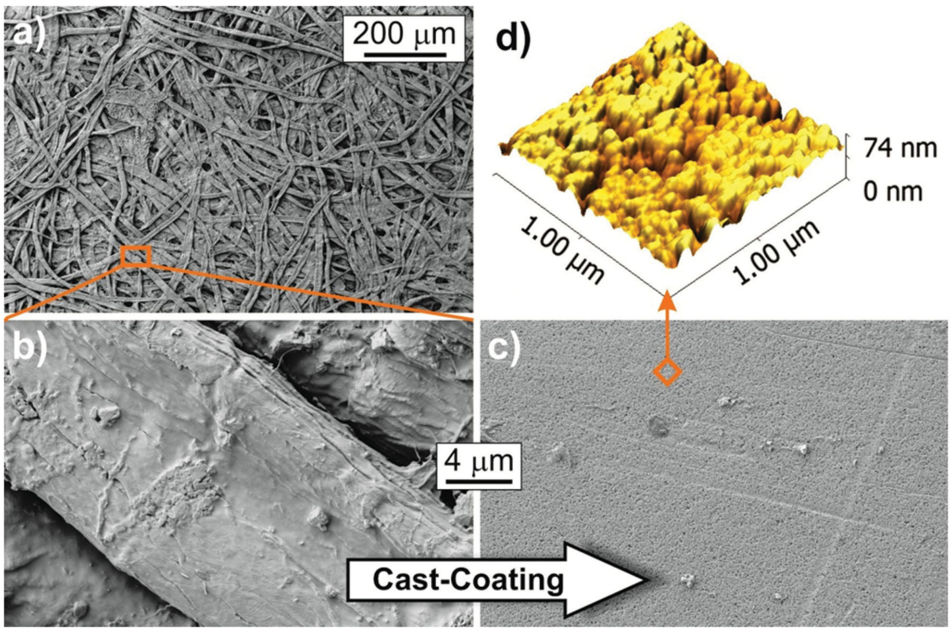

Figure 2. SEM images of the raw paper at a a) low and b) high magnifications, showing its fibrous morphology. c) SEM image of the same paper after the cast coating process at the same magnification as (b), where a hydrophilic mesoporous (HM) surface is observed. d) AFM image of the HM surface, where the nanoscale porosity is observed, with an RMS roughness of 9.42 nm.

surface, making it also adequate for use with printing techniques. Besides, its nanoscopic roughness is highly compatible with the deposition methods used to fabricate the PV device, as uniform layers are expected.

2.2. Paper Thermal Analysis

Thermo gravimetry/differential scanning calorimetry (TG/DSC) analysis results of the FS-2 paper are shown in **Figure 3**. An endothermic peak is detected at 84 °C, with a corresponding weight loss of 3.7% and an energy absorption of 55.25 J g^{-1}, which has been associated with water vapor desorption. Above this temperature, the paper shows no further mass variation up to ≈280 °C. At 339 °C a strong endothermic peak appears, causing a mass variation of 70% associated with the decomposition of the paper.[41] These results indicate that the FS-2 paper is thermally stable at least up to 250 °C.

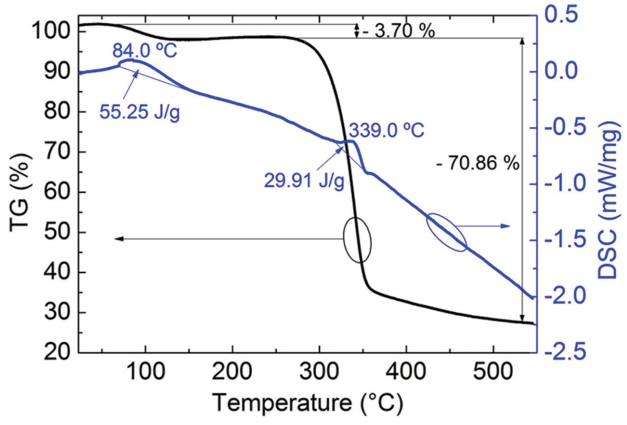

Figure 3. TG/DSC results of the FS-2 paper, where two endothermic peaks are observed at 84 °C and 339 °C, with corresponding mass variations of –3.70% and –70.56%.

2.3. Paper and Chamber Gas Desorption Analysis

Quadrupole mass spectrometry (QMS) is a useful tool for analyzing the gas desorption elements from the deposition chambers and samples, before and during the plasma deposition processes, providing complete information about the gas phase chemical composition. QMS measurements performed on glass and HN paper after 120 min in high vacuum at 250 °C are shown in **Figure 4**. Comparing both substrates, the most remarkable differences are visible in the 17–18 and 28–31 amu ranges. The 17–18 amu range is associated with water vapor release from the chamber walls and the substrate. These bands are higher for the FS-2 paper, as expected, but are still relatively low (partial pressure < 5×10^{-7} mbar). Concerning the 28–31 amu range, several group molecules can be associated with the observed bands: 28 (N_2, C_2H_4), 29 (C_2H_5), 30 (C_2H_6), 31 (CH_3O). These bands, in spite of being more intense for the FS-2 paper, are still associated with a relatively low partial pressure (< 3×10^{-8} mbar). The presence of these carboxyl groups has been attributed to the decomposition of weakly bonded molecules and monomers.[42] Since their partial pressure is still very low, and considering that the measurements were performed at a temperature much higher than that of the amorphous films deposition (150 °C), no significant contamination is expected to come from the paper during the deposition of the a-Si:H layers.

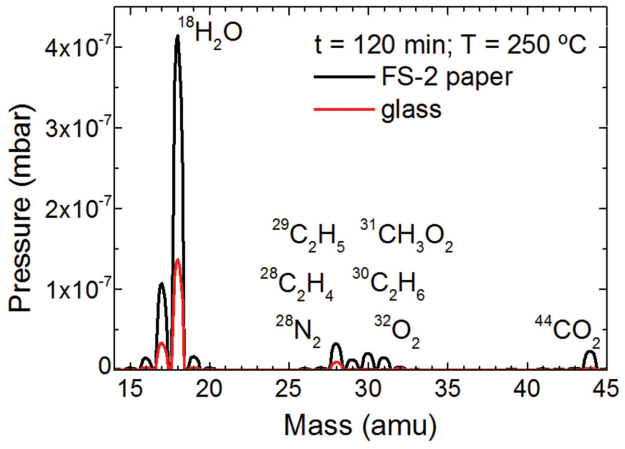

Figure 4. Quadrupole mass spectrometry (QMS) of the FS-2 paper and glass substrates obtained in vacuum at 250 °C, in the 15–45 amu range, with the corresponding identification of bands.

3. Photovoltaic Cell Characterization

3.1. Morphological Analysis

To determine the influence of the a-Si:H deposition temperature (150 °C) on the FS-2 paper surface morphology, SEM analyses of the paper surface, after heating in vacuum at 150 °C, have been performed (**Figure 5**a,b). The results show that the HM surface suffers a slight modification, becoming denser, with a reduction of mesopores density and size, resulting in a better smoothness and compactness. This modification is in good agreement with the TG/DSC analysis of the FS-2 paper, where the mass reduction and energy absorption have been associated with water vapor desorption and the densification of the surface. The SEM images of the PV device layers deposited on this surface are presented in Figure 5c–e, which show, respectively, the bottom contact Al/Ag layer, the top of the amorphous silicon (n–i–p) layers, and the top contact an amorphous IZO[21] layer. These images show that the HM surface of the FS-2 paper is suitable for the deposition of the PV device layers, as they present their typical morphology apparently free from any morphological defects (e.g., porosity). However, it should be emphasized that the intrinsic characteristics of the paper are retained, such as flexibility, allowing the deposited devices to be flexed.

A key to this breakthrough is the adherence and conformability of the first metallic layers deposited on the HM surface, where a clean and dense microcrystalline metallic layer is formed. This is evidenced by the SEM image in Figure 5c, in which a compact microcrystalline morphology is observed, typical of these metal layers and identical to those formed on glass substrates. Since deposition methods employed for the a-Si:H cells fabrication do not involve exposing the substrate to temperatures above 150 °C or solvents, the integrity of the FS-2 paper is preserved. Consequently, the a-Si:H layers deposited on the top of the Ag layer (Figure 5d) also look identical to a similar deposition performed with a glass substrate. The a-Si:H surface appears compact and free from cracks or other defects. The same is true for the top contact IZO layer (Figure 5e) where its characteristic amorphous morphology is observed. The cross section of the PV cell can be observed in the SEM image in Figure 5f. The cell layers appear compact and well defined, indicative of the good quality of the deposition.

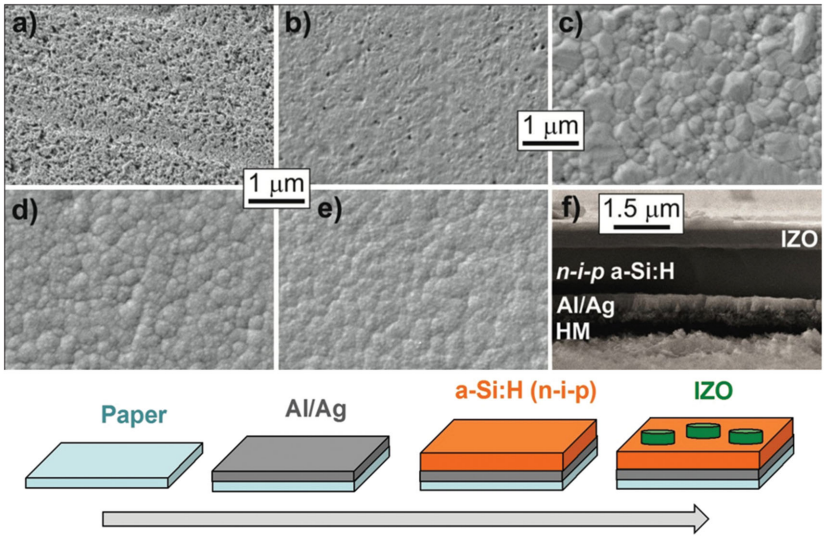

Figure 5. SEM images and schematic showing the evolution the paper cell morphology at its different fabrication stages: a) hydrophilic mesoporous (HM) paper surface before annealing; b) HM surface after annealing in vacum at 150 °C; c) Al/Ag layer deposited on the HM paper after annealing; d) a-Si:H (n–i–p) layers deposited on the Al/Ag layer; e) IZO layer deposited on the top of the a-Si:H; f) cross section of the cell, where it can be observed that all the layers and interfaces are well defined.

3.2. Electrical Characterization

Figure 6 shows the measured current density–voltage (*J*–*V*) curves of the a-Si:H PV cells deposited on a glass reference substrate and on the FS-2 paper at 150 °C, under Air Mass 1.5 (AM1.5) conditions. The cell's characteristics, extracted from the *J*–*V* curves, are shown in **Table 1**. For the cells deposited on the FS-2 paper, the best total power conversion efficiency obtained for a 5 mm^2 cell was η = 3.40%, with a fill factor FF = 40.7%, an open-circuit voltage V_{OC} = 0.82 V, and a short-circuit current density J_{SC} = 10.19 mA cm^{-2}. When compared to the cell deposited on a glass substrate during the same run, we observe predominantly a decrease in J_{SC} (–8.6%) and FF (–8.9%), which can be associated with a larger series resistance, R_S, of the paper cell. As the IZO layer was deposited through a mechanical mask, which defines the cell area, a small shadow effect at the borders of the cell's top contact is visible. However, there is no change in V_{OC} between cells, and the shunt resistance, R_{Sh}, is nearly

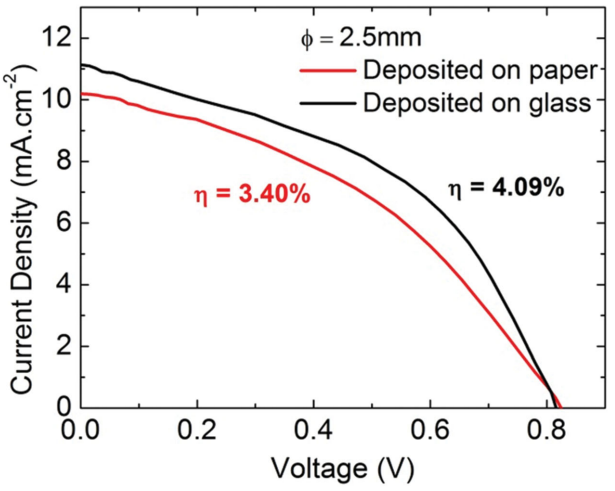

Figure 6. *J–V* characteristic curves of the cells on paper and glass with a 2.5 mm diameter under AM1.5 illumination conditions, and their respective efficiency (η). Extracted parameters are indicated in Table 2.

identical. These results, in particular the nearly identical values of V_{OC} and R_{Sh} between paper and glass cells, suggest that the electronic properties of the silicon layers' should be similar for both cells. The differences observed for the R_S of the cells can be, therefore, attributed to small thickness variation of the IZO layer affecting its sheet resistance, but also to the flexibility of the paper substrate that can induce some stress on the contact layers. Still, the cells on the FS-2 paper resisted to manual bending tests to 20 mm radius and were fully functional afterward. We thus conclude that the FS-2 paper can be successfully applied as a substrate for a-Si:H PV cells deposition with a minimal effect on their performance when compared to identical cells deposited on glass. Besides proving the concept, these results also open the path for further optimization, in particular of the layers thicknesses to better suit the paper characteristics.

Spatial distribution maps of the individual working cells performance were also performed to gain insight into the cells overall spatial process yield. The cells' *J–V* curves on the FS-2 paper substrate show a very small deviation, with the devices achieving similar V_{oc} (0.80–0.82 V). Although the cells with smaller area seem to perform better, the average variations observed (±15% overall 40 × 40 mm substrate area mapped) can also be attributed to errors associated with the real active collecting area,[43] but confirms that the paper surface is absent of defects capable of causing failures during the cells' layers deposition.

4. Conclusion and Future Perspectives

The fabrication of photovoltaic cells on paper as a proof of concept was successfully demonstrated. Efficiencies above 3% were achieved, with a nonfully optimized n–i–p configuration. Some shortcomings have been identified, and it is likely that shortly this type of light harvesting devices for indoor applications will attain the typical 6%–8% efficiencies of amorphous silicon cells with the advantages of low cost, flexibility, and large-scale production using roll-to-roll processes, more than enough to power smart labels, food sensing electronics, or to promote data communication. The cells integration can easily be achieved using ultrathin flexible masks, without the need of expensive laser lithography or photolithography. Furthermore, the cell architecture and fabrication process are compatible with the application of distinct light trapping schemes,[44,45] which allow further enhancement of the devices efficiency toward a 10% goal.

However, for their final deployment, these lightweight devices will require a flexible thin film encapsulation to achieve sufficiently long lifetimes and provide other environmental protections. There are many simple, passive, and flexible thin film encapsulation techniques that can significantly improve cell lifetimes and provide other unique protective benefits, while maintaining the pliability and paper-like qualities of the cell devices.[27] In particular, some groups[46] have recently shown the possibility of fabricating transparent paper from nanocellulose, which can be used as a protective encapsulation layer in alternative to polymers. These novel transparent papers have remarkable optical properties, such as antireflection coating (ARC) properties[47] that also produce a broadband, angle-insensitive light dispersion, which results from the incoherent scattering associated with the texture of the cellulose material, making it a promising encapsulation material for light harvesting in indoor applications.

The development of PV cell devices supported on paper may lead to a new era of flexible optoelectronic devices that are amenable to roll-to-roll deposition techniques. The light weight and flexibility of these devices can be advantageous in reducing their installation cost and opening new venues for applications, in particular the indoors ones.

5. Experimental Section

Paper Processing: The base raw paper was coated on the front and back face with a coating mass consisting of a styrene acrylate binding agent and a pigment mixture formed from calcium carbonate and kaolin

Table 1. Diameter, ϕ, efficiency, η, short-circuit current density, J_{SC}, open-circuit voltage, V_{OC}, fill factor, FF, shunt resistance, R_{Sh}, and series resistance, R_S, extracted from the *J–V* curves of the cells.

Substrate	ϕ [mm]	η [%]	J_{SC} [mA cm^{-2}]	V_{OC} [V]	FF [%]	R_{Sh} [Ω cm^2]	R_S [Ω cm^2]
Glass	2.5	4.09	11.15	0.82	44.7	175	26.9
Paper	2.5	3.40	10.19	0.82	40.7	184	41.4
Paper	2.5	3.36	9.95	0.82	41.2	117	42.1
Paper	5	2.58	8.12	0.82	38.7	201	54.1
Paper	5	2.57	7.82	0.80	41.1	240	49.3

with a coat weight of 30 g m^{-2} (front face) and 20 g m^{-2} (back face), and then dried and subsequently smoothed using a calender. The paper was then coated with a mass consisting of 80 parts boehmite pigment, ten parts pyrogenic aluminum oxide pigment, eight parts polyvinyl alcohol, and two parts boric acid, and then dried. After rewetting, the paper surface was pressed to a heated mirror gloss drum and dried again to obtain a smooth and glossy surface finish. The dry coat weight was 20 g m^{-2}; the mean pore size of the layer, measured using mercury porosimetry, was 30 nm.

Films Processing: The FS-2 paper with a thickness of 205 µm and a weight of 200 g m^{-2} was cut into pieces of 5 × 10 cm and attached to a 1 mm thick glass substrate using polyamide tape for ease of manipulation and deposition of the cell layers, since roll-to-roll deposition equipment was not available in our laboratory. Prior to any deposition, the paper was annealed in vacuum at 150 °C for 30 min. The PV device consisted of the structure: Al/Ag/a-Si:H(n)/a-Si:H(i)/a-Si:H(p)/IZO. A layer of Al/Ag was used for the back contact, with thicknesses of 80 and 40 nm, respectively, deposited in vacuum by thermal resistive evaporation from a base pressure of 3×10^{-6} Torr. The n–i–p hydrogenated amorphous silicon (a-Si:H) cell structure was deposited by PECVD in a cluster deposition chamber, where the layers were deposited in individual chambers to avoid cross contamination from dopant gases, and where the substrate was allowed to move between each deposition chamber without breaking the vacuum. The a-Si:H layers deposition conditions were the following: substrate temperature, 150 °C; base pressure, 2×10^{-7} Torr; prior to deposition of each layer the chambers were purged with Argon for 5 min for decontamination of volatile elements released by the paper. Before starting each layer, the deposition chamber temperature was homogenized with a small H_2 flux at the deposition pressure; the total cell deposition time was 1 h and 40 min; the remaining deposition conditions are summarized in **Table 2**. For the top contact, an amorphous indium zinc oxide (IZO) transparent conductive oxide (TCO) with 200 nm was deposited by RF magnetron sputtering from an IZO target at room temperature. A polyimide mechanical mask with open circles with 2.5 and 5 mm of diameter was used to define the cells' area. The system base pressure was 3×10^{-6} Torr. The deposition power was raised slowly in steps of 160 mW cm^{-2} (5 min), 220 mW cm^{-2} (10 min), 275 mW cm^{-2} (10 min), and 412 mW cm^{-2} (35 min) in order to avoid damage of the silicon layers with the TCO deposition. The O_2 and Ar partial pressures were, respectively, 1.9×10^{-5} and 2×10^{-3} mbar. In view of increasing the throughput of the fabrication process, the present growth rate can be further enhanced in future upscale by increasing the deposition frequency using variable high-frequency (VHF) PECVD and/or increasing the deposition pressure and power with proper H_2 dilution ratio, keeping the same growth surface processes.[38,40]

Characterization Techniques: Scanning electron microscopy (SEM) observations were carried out in a Carl Zeiss AURIGA CrossBeam (FIB-SEM) workstation in the secondary electron image mode. Atomic force microscopy (AFM) measurements were performed in ac mode with an Asylum MFP3D to determine the HN paper surface roughness. Thermogravimetric analysis (TGA) and differential scanning calorimetry (DSC) were carried out in a simultaneous thermal analyzer (TGA-DSC-STA 449 F3 Jupiter). Approximately 7.5 mg of each sample was loaded into an aluminum pan and heated from 25 to 550 °C with a heating rate of 5 °C min^{-1}. All the measurements were performed under ambient atmosphere. Quadrupole mass spectrometry (QMS) data were collected using the mass spectrometry system (EXtorr, model XT100M) connected to the PECVD system, before deposition of the device layers, to determine the contamination arising from the paper substrate compared to a conventional glass substrate. The mass spectrometer was mounted parallel to the process chamber exhaust line and exhaust gases were collected through a 10 µm sampling orifice located 500 cm away from the outer edge of the RF electrode, for a detection mass range up to 100 amu. QMS data were collected after 120 min of chamber pumping with a temperature of 250 °C. The solar cells were characterized by current–voltage (*J–V*) measurements at room temperature under AM1.5 (100 mW cm^{-2}) light conditions in a Spire Sun Simulator 240A.

Table 2. Amorphous silicon layers thickness and deposition conditions: hydrogen dilution, D_H (%); dopant (trimethilboron or phosphine) ratio to silane, R_d (%); deposition pressure (Torr); power density, P_d (mW cm^{-2}); plasma excitation frequency, P_f (MHz).

Layer	Thickness [nm]	D_H [%]	R_d [%]	Pressure [Torr]	P_d [mW cm^{-2}]	P_f [MHz]
N	35	67	3.0	1.00	21	13.56
I	300	50	–	0.50	69	30.00
P	20	58	1.6	0.65	21	13.56

Supporting Information

Supporting Information is available from the Wiley Online Library or from the author.

Acknowledgements

This work was partially supprted by FEDER funds through the COMPETE 2020 Programme and National Funds throught FCT - Portuguese Foundation for Science and Technology under the projects UID/CTM/50025/2013; EXCL/CTM-NAN/0201/2012; EXPL/CTM-NAN/1184/2013 and A3Ple (FP7, NMP-2010-SME-4 Grant 262782). This work was also supported by E.F.'s ERC 2008 Advanced Grant (INVISIBLE Contract Number 228144).The authors want to thank their colleagues Daniela Gomes for SEM images acquisition, and Tomás Clameiro for the AFM Measurements. A.V. acknowledges the support from the Portuguese Foundation for Science and Technology (FCT) and MIT-Portugal through the scholarship SFRH/BD/33978/2009. D.G. acknowledges the support from the Portuguese Foundation for Science and Technology through the Advatech PhD program scholarship PD/BD/52627/2014;. M.J.M. acknowledges funding by the EU Marie Curie Action FP7-PEOPLE-2013-IEF through the DIELECTRIC PV project (Grant No. 629370).

Received: February 14, 2015
Revised: April 13, 2015
Published online: May 7, 2015

[1] R. Martins, L. Pereira, E. Fortunato, *Inf. Disp.* **2014**, *30*, 4.
[2] R. Martins, I. Ferreira, E. Fortunato, *Phys. Status Solidi (RRL) Rapid Res. Lett.* **2011**, *5*, 332.
[3] J.-W. Han, B. Kim, J. Li, M. Meyyappan, *J. Phys. Chem. C* **2012**, *116*, 22094.
[4] I. Ferreira, B. Bras, N. Correia, P. Barquinha, E. Fortunato, R. Martins, *J. Disp. Technol.* **2010**, *6*, 332.
[5] I. Ferreira, B. Brás, J. I. Martins, N. Correia, P. Barquinha, E. Fortunato, R. Martins, *Electrochim. Acta* **2011**, *56*, 1099.
[6] M. Jorgensen, K. Norrman, S. A. Gevorgyan, T. Tromholt, B. Andreasen, F. C. Krebs, *Adv. Mater.* **2012**, *24*, 580.
[7] M.-C. Choi, Y. Kim, C.-S. Ha, *Prog. Polym. Sci.* **2008**, *33*, 581.
[8] A. Shah, P. Torres, R. Tscharner, N. Wyrsch, H. Keppner, *Science* **1999**, *285*, 692.
[9] S. F. Leung, L. Gu, Q. Zhang, K. H. Tsui, J. M. Shieh, C. H. Shen, T. H. Hsiao, C. H. Hsu, L. Lu, D. Li, Q. Lin, Z. Fan, *Sci. Rep.* **2014**, *4*, 4243.
[10] H. Sirringhaus, *Adv. Mater.* **2014**, *26*, 1319.
[11] Y. Fujisaki, H. Koga, Y. Nakajima, M. Nakata, H. Tsuji, T. Yamamoto, T. Kurita, M. Nogi, N. Shimidzu, *Adv. Funct. Mater.* **2014**, *24*, 1657.
[12] S.-I. Na, S.-S. Kim, J. Jo, D.-Y. Kim, *Adv. Mater.* **2008**, *20*, 4061.

[13] T. R. Andersen, H. F. Dam, B. Andreasen, M. Hösel, M. V. Madsen, S. A. Gevorgyan, R. R. Søndergaard, M. Jørgensen, F. C. Krebs, *Solar Energy Mater. Solar Cells* **2014**, *120*, 735.
[14] D. Tobjork, R. Osterbacka, *Adv. Mater.* **2011**, *23*, 1935.
[15] T.-S. Kim, S.-I. Na, S.-S. Kim, B.-K. Yu, J.-S. Yeo, D.-Y. Kim, *Phys. Status Solidi (RRL) Rapid Res. Lett.* **2012**, *6*, 13.
[16] G. Zhou, F. Li, H.-M. Cheng, *Energy Environ. Sci.* **2014**, *7*, 1307.
[17] L. Pereira, D. Gaspar, D. Guerin, A. Delattre, E. Fortunato, R. Martins, *Nanotechnology* **2014**, *25*, 094007.
[18] H. Zhu, Z. Fang, C. Preston, Y. Li, L. Hu, *Energy Environ. Sci.* **2014**, *7*, 269.
[19] U. Zschieschang, T. Yamamoto, K. Takimiya, H. Kuwabara, M. Ikeda, T. Sekitani, T. Someya, H. Klauk, *Adv. Mater.* **2011**, *23*, 654.
[20] G. Zheng, Y. Cui, E. Karabulut, L. Wågberg, H. Zhu, L. Hu, *MRS Bull.* **2013**, *38*, 320.
[21] E. Fortunato, N. Correia, P. Barquinha, L. Pereira, G. Goncalves, R. Martins, *IEEE Electron. Device Lett.* **2008**, *29*, 988.
[22] P. Andersson, D. Nilsson, P. O. Svensson, M. X. Chen, A. Malmstrom, T. Remonen, T. Kugler, M. Berggren, *Adv. Mater.* **2002**, *14*, 1460.
[23] A. C. Siegel, S. T. Phillips, M. D. Dickey, N. Lu, Z. Suo, G. M. Whitesides, *Adv. Funct. Mater.* **2010**, *20*, NA.
[24] R. F. P. Martins, A. Ahnood, N. Correia, L. M. N. P. Pereira, R. Barros, P. M. C. B. Barquinha, R. Costa, I. M. M. Ferreira, A. Nathan, E. E. M. C. Fortunato, *Adv. Funct. Mater.* **2013**, *23*, 2153.
[25] J. H. Kim, S. Mun, H. U. Ko, G. Y. Yun, J. Kim, *Nanotechnology* **2014**, *25*, 092001.
[26] M. N. Costa, B. Veigas, J. M. Jacob, D. S. Santos, J. Gomes, P. V. Baptista, R. Martins, J. Inacio, E. Fortunato, *Nanotechnology* **2014**, *25*, 094006.
[27] M. C. Barr, J. A. Rowehl, R. R. Lunt, J. Xu, A. Wang, C. M. Boyce, S. G. Im, V. Bulovic, K. K. Gleason, *Adv. Mater.* **2011**, *23*, 3499.
[28] Z. Fang, H. Zhu, Y. Yuan, D. Ha, S. Zhu, C. Preston, Q. Chen, Y. Li, X. Han, S. Lee, G. Chen, T. Li, J. Munday, J. Huang, L. Hu, *Nano Lett.* **2014**, *14*, 765.
[29] A. D. Mazzeo, W. B. Kalb, L. Chan, M. G. Killian, J. F. Bloch, B. A. Mazzeo, G. M. Whitesides, *Adv. Mater.* **2012**, *24*, 2850.
[30] H. Águas, S. K. Ram, A. Araújo, D. Gaspar, A. Vicente, S. A. Filonovich, E. Fortunato, R. Martins, I. Ferreira, *Energy Environ. Sci.* **2011**, *4*, 4620.
[31] Y. Zhou, T. M. Khan, J.-C. Liu, C. Fuentes-Hernandez, J. W. Shim, E. Najafabadi, J. P. Youngblood, R. J. Moon, B. Kippelen, *Org. Electron.* **2014**, *15*, 661.
[32] Y. Zhou, C. Fuentes-Hernandez, T. M. Khan, J. C. Liu, J. Hsu, J. W. Shim, A. Dindar, J. P. Youngblood, R. J. Moon, B. Kippelen, *Sci. Rep.* **2013**, *3*, 1536.
[33] a) R. Martins, L. Raniero, L. Pereira, D. Costa, H. Águas, S. Pereira, L. Silva, A. Gonçalves, I. Ferreira, E. Fortunato, *Phil. Mag.* **2009**, *89*, 2699; b) A. V. Shah, H. Schade, M. Vanecek, J. Meier, E. Vallat-Sauvain, N. Wyrsch, U. Kroll, C. Droz, J. Bailat, *Prog. Photovoltaics Res. Appl.* **2004**, *12*, 113.
[34] S. W. B.-G. Kirsten, *US2012234585(A1)* **2012**.
[35] P. Ihalainen, A. Määttänen, J. Järnström, D. Tobjörk, R. Österbacka, J. Peltonen, *Ind. Eng. Chem. Res.* **2012**, *51*, 6025.
[36] D.-H. Kim, Y.-S. Kim, J. Wu, Z. Liu, J. Song, H.-S. Kim, Y. Y. Huang, K.-C. Hwang, J. A. Rogers, *Adv. Mater.* **2009**, *21*, 3703.
[37] R. Street, *Hydrogenated Amorphous Silicon*, Cambridge University Press, Cambridge **1991**.
[38] M. Izu, T. Ellison, *Solar Energy Mater. Solar Cells* **2003**, *78*, 613.
[39] S.-Y. Lo, D.-S. Wuu, C.-H. Chang, C.-C. Wang, S.-Y. Lien, R.-H. Horng, *IEEE Trans. Electron Devices* **2011**, *58*, 1433.
[40] F. Qi, H. Guofu, L. Xianbo, X. Xianbi, C. Changyong, I. William, N. Adiga, S. Zhang, X. Cao, W. Du, X. Deng, in *Photovoltaic Specialists Conf. (PVSC), 2010 35th IEEE* **2010**, 001491, DOI: 10.1109/PVSC.2010.5614457.
[41] T. Andersson, B. Stalbom, B. Wesslen, *J. Appl. Polym. Sci.* **2004**, *91*, 1525.
[42] I. Milosavljevic, E. M. Suuberg, *Ind. Eng. Chem. Res.* **1995**, *34*, 1081.
[43] R. Martins, E. Fortunato, *J. Appl. Phys.* **1995**, *78*, 3481.
[44] M. J. Mendes, S. Morawiec, F. Simone, F. Priolo, I. Crupi, *Nanoscale* **2014**, *6*, 4796.
[45] S. Morawiec, M. J. Mendes, S. A. Filonovich, T. Mateus, S. Mirabella, H. Aguas, I. Ferreira, F. Simone, E. Fortunato, R. Martins, F. Priolo, I. Crupi, *Opt. Express* **2014**, *22 Suppl 4*, A1059.
[46] D. Gaspar, S. N. Fernandes, A. G. de Oliveira, J. G. Fernandes, P. Grey, R. V. Pontes, L. Pereira, R. Martins, M. H. Godinho, E. Fortunato, *Nanotechnology* **2014**, *25*, 094008.
[47] D. Ha, Z. Fang, L. Hu, J. N. Munday, *Adv. Energy Mater.* **2014**, *4*, 1301804.